

All figures in the manuscript

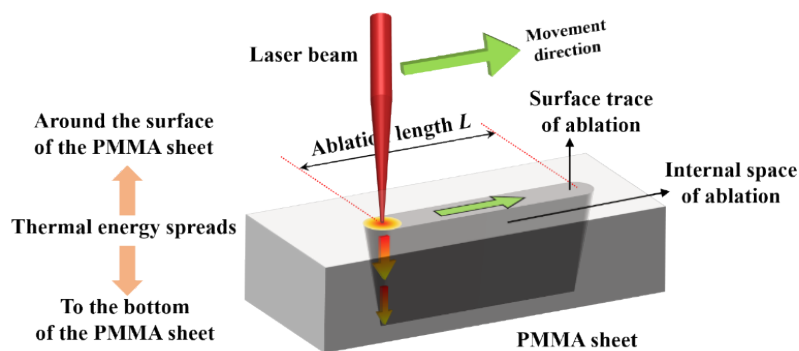


Figure S1 Schematic diagram of physical phenomena during laser ablation process.

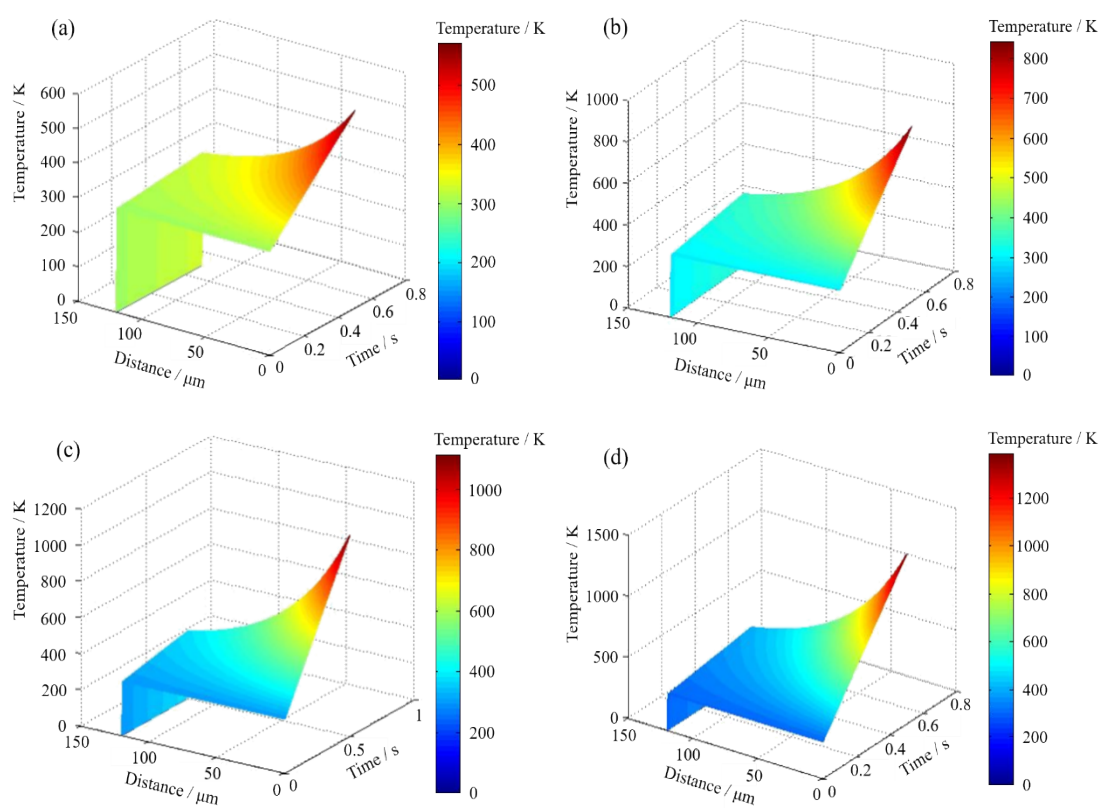


Figure S2 Temperature changes in the CO₂ continuous laser dressing PMMA material. (a) Laser power: 20 W, velocity: 90 mm/s; (b) Laser power: 40 W, velocity: 90 mm/s; (c) Laser power: 60 W, velocity: 90 mm/s; (d) Laser power: 80 W, velocity: 90 mm/s.

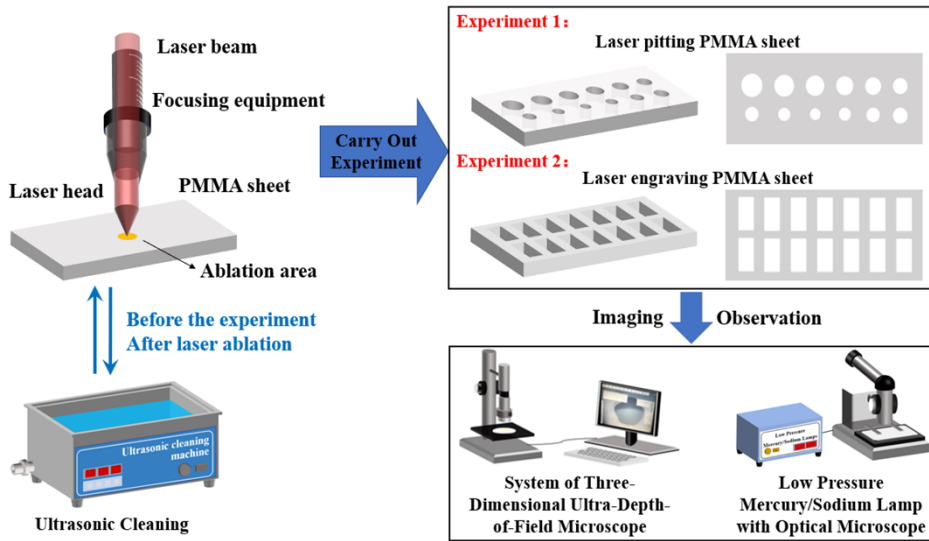


Figure S3 Experiment process flow chart of continuous laser ablation of PMMA material.

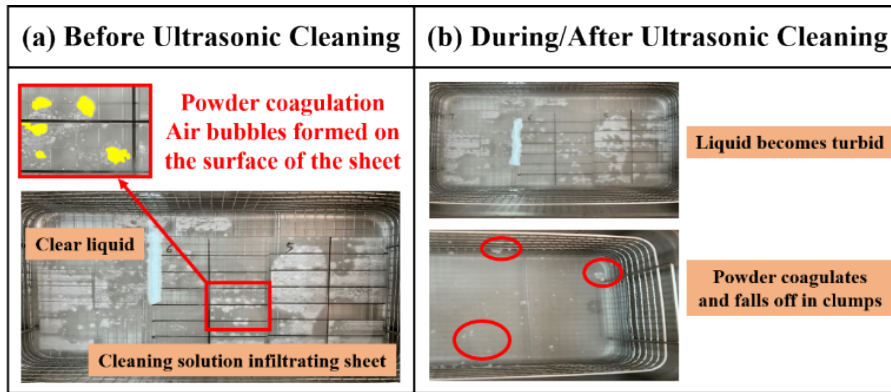


Figure S4 Comparison of ultrasonic cleaning effects.

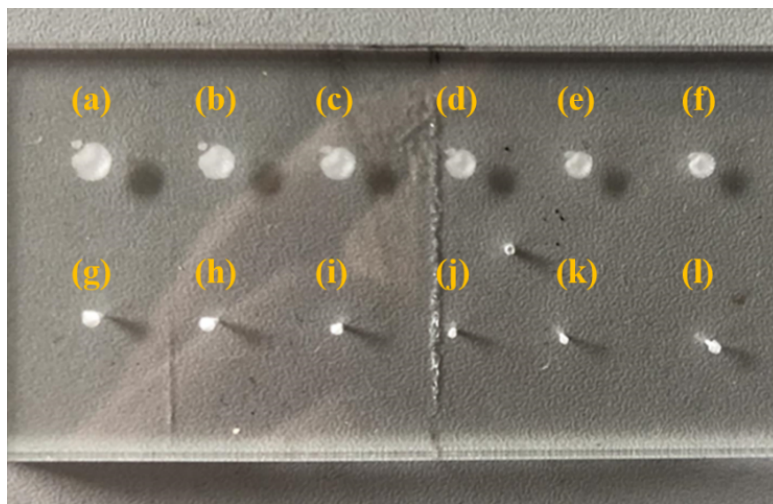


Figure S5 PMMA sheet after CO₂ continuous laser shot where the defocusing distance is (a) 14 mm; (b) 12 mm; (c) 10 mm; (d) 8 mm; (e) 6 mm;

(f) 4 mm; (g) 2 mm; (h) 0 mm; (i) -2 mm; (j) -4 mm; (k) -6 mm; (l) -8 mm.

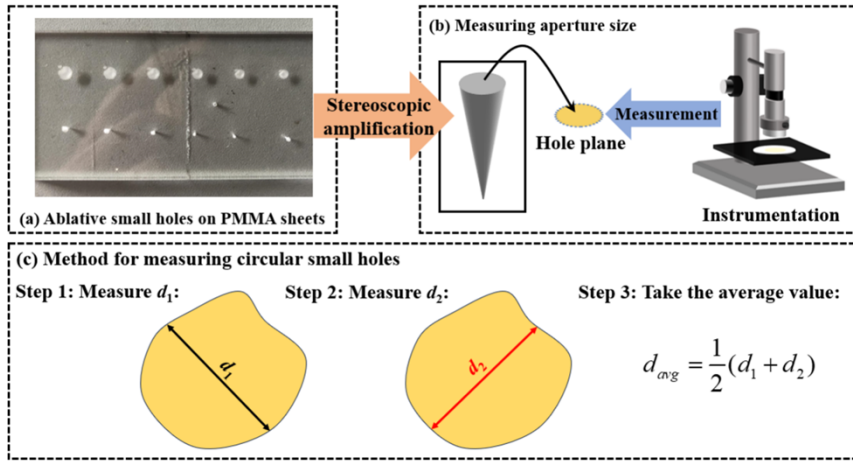


Figure S6 Method for measuring circular small holes.

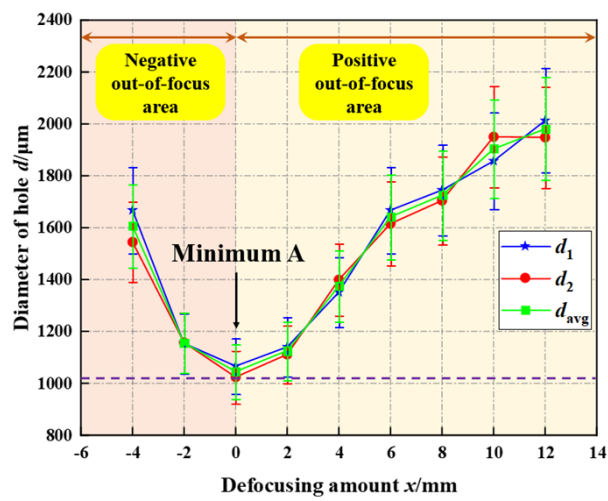
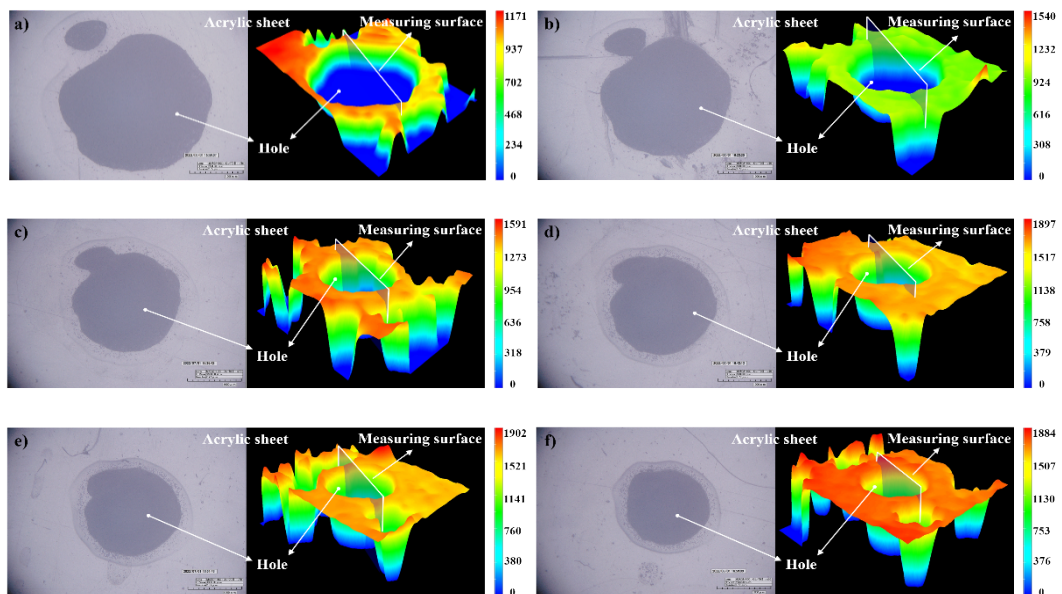


Figure S7 Variation law of the diameter of the small hole with the defocusing amount.



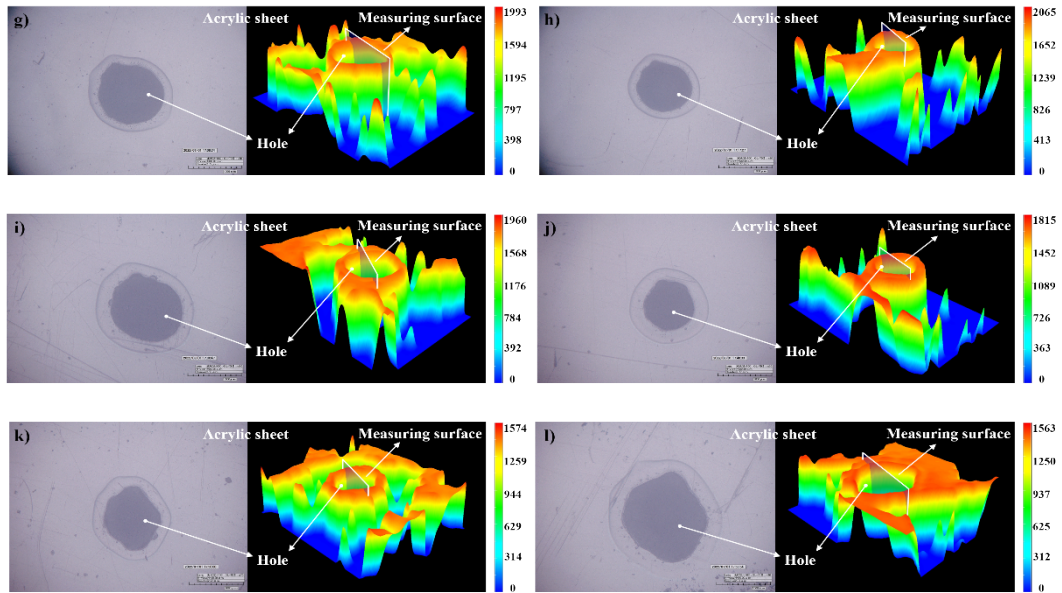


Figure S8 Surface topography map of continuous laser ablation of PMMA material where the defocusing distance is (a) 14 mm; (b) 12 mm; (c) 10 mm; (d) 8 mm; (e) 6 mm; (f) 4 mm; (g) 2 mm; (h) 0 mm; (i) -2 mm; (j) -4 mm; (k) -6 mm; (l) -8 mm.

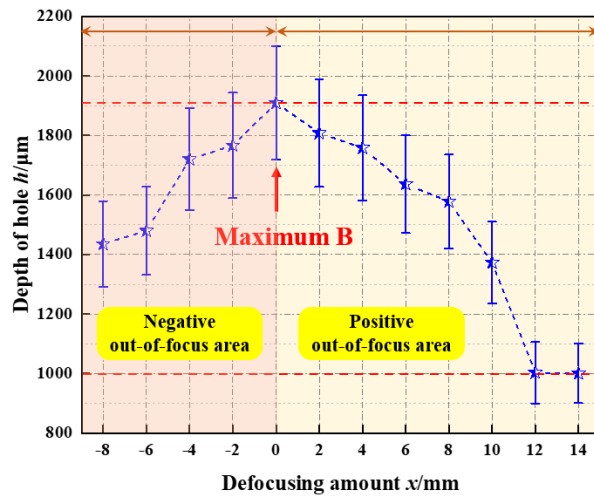


Figure S9 Variation law of the hole depth with the defocus amount.

Laser power density (W/mm^2) 23.3	Velocity (mm/s)	30	60	90
	Interior	(1)	(3)	(5)
Margin	(2)	(4)	(6)	

Figure S10 Surface morphology of PMMA sheet observed under low-pressure mercury/sodium lamp with optical microscope.

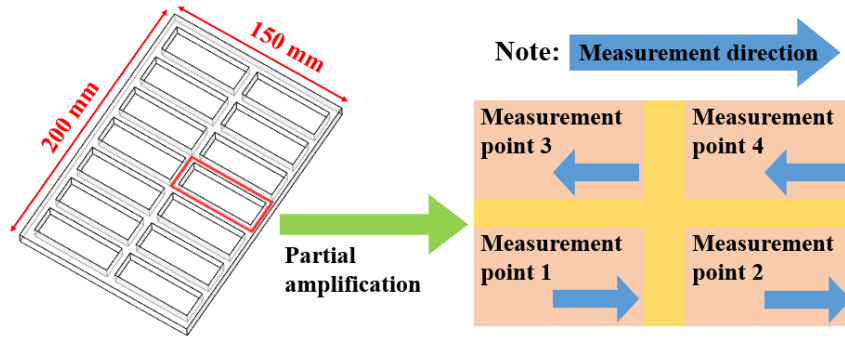


Figure S11 Schematic diagram of surface roughness measuring device.

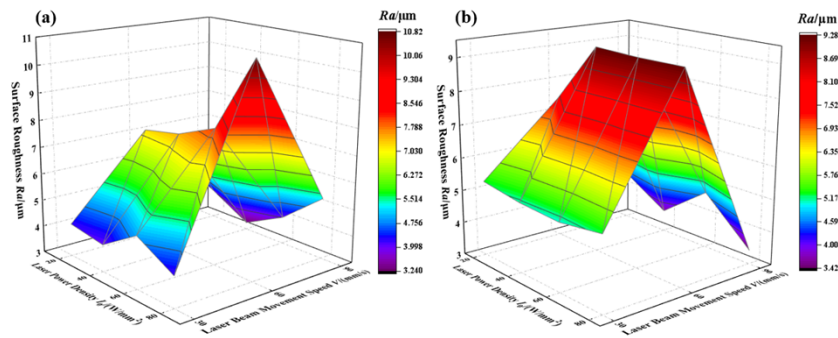


Figure S12 Variation law of surface roughness value (Ra) with laser power density and laser beam movement velocity.

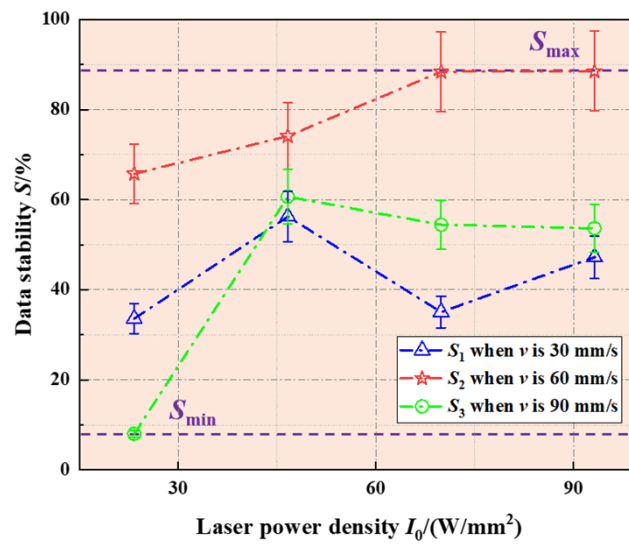


Figure S13 Variation law of data stability with laser power density and laser beam movement velocity.

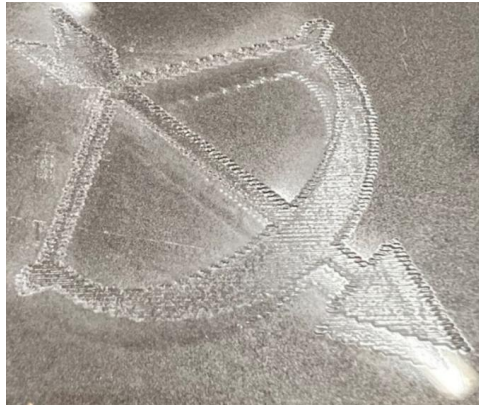


Figure S14 CO₂ continuous laser ablation of PMMA material process samples.

Processing parameters	Before Ultrasonic Cleaning	After Ultrasonic Cleaning
Laser power density 20 W/mm ² Laser beam movement speed 30 mm/s		
Laser power density 20 W/mm ² Laser beam movement speed 60 mm/s		
Laser power density 20 W/mm ² Laser beam movement speed 90 mm/s		

(a) Laser power density of 23.3 W/mm²

Processing parameters	Before Ultrasonic Cleaning	After Ultrasonic Cleaning
Laser power density 60 W/mm ² Laser beam movement speed 30 mm/s		
Laser power density 60 W/mm ² Laser beam movement speed 60 mm/s		
Laser power density 60 W/mm ² Laser beam movement speed 90 mm/s		

(c) Laser power density of 69.9 W/mm²

Processing parameters	Before Ultrasonic Cleaning	After Ultrasonic Cleaning
Laser power density 40 W/mm ² Laser beam movement speed 30 mm/s		
Laser power density 40 W/mm ² Laser beam movement speed 60 mm/s		
Laser power density 40 W/mm ² Laser beam movement speed 90 mm/s		

(b) Laser power density of 46.6 W/mm²

Processing parameters	Before Ultrasonic Cleaning	After Ultrasonic Cleaning
Laser power density 80 W/mm ² Laser beam movement speed 30 mm/s		
Laser power density 80 W/mm ² Laser beam movement speed 60 mm/s		
Laser power density 80 W/mm ² Laser beam movement speed 90 mm/s		

(d) Laser power density of 93.2 W/mm²

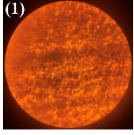
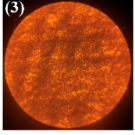
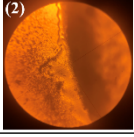
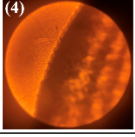
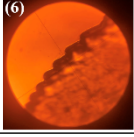
Figure S15 Ultrasonic cleaning effect under different laser process parameters.

Laser power density (W/mm ²)	Velocity (mm/s)	30	60	90
	23.3	Interior		
Margin				

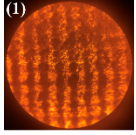
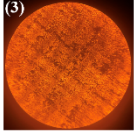
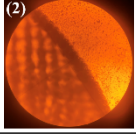
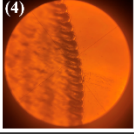
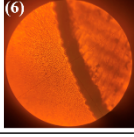
(a) Laser power density of 23.3 W/mm²

Laser power density (W/mm ²)	Velocity (mm/s)	30	60	90
	49.6	Interior		
Margin				

(b) Laser power density of 46.6 W/mm²

Laser power density (W/mm ²) 69.9	Velocity (mm/s)	30	60	90
	Interior		(1) 	(3) 
Margin		(2) 	(4) 	(6) 

(c) Laser power density of 69.9 W/mm²

Laser power density (W/mm ²) 93.2	Velocity (mm/s)	30	60	90
	Interior		(1) 	(3) 
Margin		(2) 	(4) 	(6) 

(d) Laser power density of 93.2 W/mm²

Figure S16 Surface morphology of PMMA sheet observed under low-pressure mercury/sodium lamp with optical microscope.

All tables in the manuscript

Table S1 Parameter table

Parameter content	Name	Symbol/Unit	Numerical Value	Name	Symbol/Unit	Numerical Value
Thermophysical parameters of the PMMA	Atomic mass	m/kg	1.661×10^{-25}	Specific heat capacity	$\lambda/(\text{J} \cdot \text{kg}^{-1} \cdot \text{K}^{-1})$	1420
	Density	$\rho_s/(\text{kg} \cdot \text{m}^{-3})$	1180	Melting temperature	T_m/K	403.15-413.5
	Thermal conductivity	$k_s/(\text{W} \cdot \text{m}^{-1} \cdot \text{K}^{-1})$	0.189	Gasification temperature	T_v/K	543.15
	Thermal diffusivity	$\gamma/(\text{m}^2 \cdot \text{s}^{-1})$	11×10^8	absorption coefficient	b	0.92
Calculation parameters	Laser Wavelength	λ/nm	1064	Spot diameter	$D/\mu\text{m}$	562
	Electron mass	m_e/kg	9.1×10^{-31}	Laser output power	P/W	100
	Table stroke	l/mm	1300×900	Lighting time	t/s^{-1}	0.5
	Atmospheric pressure	—	50 %	Lighting mode	—	Spotting/ablation

Table S2 Parameters of laser ablation processing

Name	Numerical values
Laser wavelength λ/nm	1064
Laser power P/W	100
Workbench stroke l/mm	1300×900
Light output time t/s	0.5
Air pressure	50%
Luminous mode	Spotting

Table S3 The diameter of the small hole after laser engraving d_1 and d_2

Defocusing amount x/mm	Diameter $d_1/\mu\text{m}$	Diameter $d_2/\mu\text{m}$
12	2013±201	1948±195
10	1857±186	1950±195
8	1744±174	1704±170
6	1667±167	1615±162
4	1351±135	1399±140
2	1140±114	1111±111
0	1066±107	1024±102
-2	1154±115	1157±116
-4	1667±167	1544±154

Table S4 Laser power density corresponding to different laser spot diameters

Defocusing amount (x)/mm	Diameter of the laser spot (d)/ μm	Laser power density (I_0)/(W/mm ²)
12	1980	32.5
10	1903	35.1
8	1724	42.8
6	1641	47.2
4	1375	67.3
2	1125	100.4
0	1045	116.5
-2	1155	95.3
-4	1606	49.3

Note: The laser power is all 100 W.

Table S5 Laser process parameters

Name	Unit	Numerical Value	Name	Unit	Numerical Value
Laser wavelength	λ /nm	1064	Laser power	P /W	20/40/60/80
Defocusing amount	x /mm	0	Laser power density	I_0 /(W.mm ⁻²)	23.3/46.6/69.9/93.2
Laser beam movement velocity	v /(mm.s ⁻¹)	20/40/60/80/100	Atmospheric pressure	—	50%
Target graphic dimensions	l /mm	70×28	Light output method	—	Engraving

Table S6 Surface roughness values under different laser process parameters

Laser power density (I_0)/(W/mm ²)	Laser beam moving velocity (v)/(mm/s)	Surface roughness values (Ra)/ μm					Average value
		Measurement point 1	Measurement point 2	Measurement point 3	Measurement point 4		
23.3	90	4.46	4.29	4.55	4.65	4.49	
46.6	90	5.00	2.85	2.78	4.00	3.66	
69.9	90	6.09	4.47	3.51	4.90	4.74	
93.2	90	4.25	3.76	2.41	3.33	3.43	

Table S7 Calculated value of data stability

Laser power density (I_0)/(W/mm ²)	Laser beam moving velocity (v)/(mm/s)	Data stability (S)/%
23.3	30	33.58
	60	65.77
	90	8.02
46.6	30	56.25
	60	74.11
	90	60.66
69.9	30	35.05
	60	88.39
	90	54.43
93.2	30	47.24
	60	88.52
	90	53.64

Table S8 Surface roughness values under different laser process parameters

Laser power density (I_0)/(W/mm ²)	Laser beam moving velocity (v)/(mm/s)	Surface roughness values (Ra)/ μ m				Average value
		Measurement point 1	Measurement point 2	Measurement point 3	Measurement point 4	
23.3	30	5.79	5.22	4.21	5.99	5.30
	60	9.89	5.02	4.99	9.89	7.45
	90	4.46	4.29	4.55	4.65	4.49
46.6	30	5.98	3.74	4.16	6.62	5.12
	60	12.41	5.54	9.82	9.33	9.27
	90	5.00	2.85	2.78	4.00	3.66
69.9	30	5.98	4.21	4.34	5.67	5.05
	60	11.44	8.33	4.48	12.63	9.22
	90	6.09	4.47	3.51	4.90	4.74
93.2	30	5.84	4.80	3.95	6.43	5.25
	60	12.05	6.59	5.06	13.23	9.23
	90	4.25	3.76	2.41	3.33	3.43

Appendixes in the manuscript

Appendix A (Formula number continues from the main text)

The derivation process of heat transfer physical model for carbon dioxide continuous laser processing of PMMA materials

If the ablation length of a continuous laser was set to L and its linear velocity of movement was v , the time for CO₂ continuous laser ablation of PMMA sheets was expressed as:

$$t = L/v \quad (5)$$

The total heat output (Q_z) during laser ablation of PMMA sheets was expressed as:

$$Q_z = tP = \frac{LP}{v} \quad (6)$$

The energy of a CO₂ continuous laser beam exhibits a Gaussian distribution in both time and space, and the laser energy density is higher in the center of the laser beam and gradually decreases along the Gaussian contour as the laser beam radius increases [14-16].

The specific expression was:

$$I_0(t) = I_0 \exp\left(-\frac{(t-\tau/2)^2}{2\sigma^2}\right) \quad (7)$$

$$q(r) = q_m \exp\left(-\frac{(r-\tau/2)^2}{2\sigma^2}\right) \quad (8)$$

The ablation distance of the laser beam on the PMMA sheet was L , and the diffusion and transfer distance of thermal energy on the ablation surface of the plate could be regarded as infinite. Therefore, when the laser beam performed L-length ablation on the PMMA sheet, the thermal energy absorbed by the plate surface was equal to the total heat output by the laser. It could be expressed as:

$$\int_0^L \int_{-\infty}^{\infty} q_m \exp\left(-\frac{(y-\tau/2)^2}{2\sigma^2}\right) dx dy = \frac{LP}{v} \quad (9)$$

$$2 \int_0^L \int_0^{\infty} q_m \exp\left(-\frac{(y-\tau/2)^2}{2\sigma^2}\right) dx dy = \frac{LP}{v} \quad (10)$$

$$2Lq_m \int_0^{\infty} \exp\left(-\frac{(y-\tau/2)^2}{2\sigma^2}\right) dy = \frac{LP}{v} \quad (11)$$

$$2\sqrt{2}Lq_m\sigma \int_0^{\infty} \exp\left(-\frac{(y-\tau/2)^2}{2\sigma^2}\right) d\left[\frac{(y-\tau/2)}{\sqrt{2}\sigma}\right] = \frac{LP}{v} \quad (12)$$

$$\sqrt{2}Lq_m\sigma \int_{-\infty}^{+\infty} \exp\left(-\frac{(y-\tau/2)^2}{2\sigma^2}\right) d\left[\frac{(y-\tau/2)}{\sqrt{2}\sigma}\right] = \frac{LP}{v} \quad (13)$$

$$Lq_m \int_{-\infty}^{+\infty} \exp\left(-\frac{(y-\tau/2)^2}{2\sigma^2}\right) d(y-\tau/2) = \frac{LP}{v} \quad (14)$$

$$\int_{-\infty}^{+\infty} \exp\left(-\frac{(y-\tau/2)^2}{2\sigma^2}\right) d(y-\tau/2) = \sqrt{2\pi\sigma^2} \quad (15)$$

$$\sqrt{2\pi}\sigma Lq_m = \frac{LP}{v} \quad (16)$$

$$q_m = \frac{P}{\sqrt{2\pi}\sigma v} \quad (17)$$

By substituting the peak expression q_m (17) into Equation (8), we can obtain:

$$q(r) = \frac{P}{\sqrt{2\pi\sigma v}} \exp\left(-\frac{(r-\tau/2)^2}{2\sigma^2}\right) \quad (18)$$

In the process of CO₂ continuous laser ablation of PMMA sheets, a filamentous Gaussian heat source term was introduced, and the influence of the linear velocity of laser beam translation was considered. Based on the coupled Fourier heat transfer basic model, a physical heat transfer model for CO₂ continuous laser ablation of PMMA sheets was established as follows [17-19]:

$$\rho c \left(\frac{\partial T}{\partial t}\right) = \frac{\partial}{\partial l} \left(k \frac{\partial T}{\partial l}\right) + b e^{-bl} \frac{P}{\sqrt{2\pi\sigma v}} \exp\left(-\frac{(r-\tau/2)^2}{2\sigma^2}\right) \quad (19)$$

In the formula, b is the absorption rate of PMMA sheet; L is the distance between the incident laser and the surface of PMMA sheet. The Initial condition was set to approximately 300 K at room temperature, the heat energy transmission at the surface of PMMA plate was the absorption of laser energy by the material surface, and there was no further heat energy transmission at the maximum ablation depth of the plate [20-22]. The initial condition and the boundary conditions were established as follows:

$$T(l, t) = T_0, \quad t = 0 \quad (20)$$

$$-k \left. \frac{\partial T}{\partial l} \right|_{l=0} = \frac{bP}{\sqrt{2\pi\sigma v}} \exp\left(-\frac{\tau^2}{8\sigma^2}\right) \quad (21)$$

$$-k \left. \frac{\partial T}{\partial l} \right|_{l=\delta} = 0 \quad (22)$$

The Finite-difference time-domain method is a numerical method for solving differential equations, which can be used to solve ordinary differential equation and partial differential equations [23,24]. Therefore, the finite difference equations for the heat transfer physical model (19) and boundary conditions (16), (17), and (18) were established as follows:

$$\rho c \frac{T_i^{j+1} - T_i^j}{\Delta t} = k \frac{T_{i+1}^j - 2T_i^j + T_{i-1}^j}{(\Delta l)^2} + \frac{bP}{\sqrt{2\pi\sigma v}} \exp(-bi\Delta l) \exp\left(-\frac{(j\Delta t - \tau/2)^2}{2\sigma^2}\right) \quad (23)$$

$$-k \frac{T_1^j - T_0^j}{\Delta l} = \frac{bP}{\sqrt{2\pi\sigma v}} \exp\left(-\frac{(j\Delta t - \tau/2)^2}{2\sigma^2}\right) \quad (24)$$

$$T_d^j = 0 \quad (25)$$

$$T_i^0 = 300 \text{ K} \quad (26)$$

After organizing Equation (23), we could obtain:

$$T_i^{j+1} = \frac{k\Delta t}{\rho c(\Delta l)^2} T_{i+1}^j + \left(1 - \frac{2k\Delta t}{\rho c(\Delta l)^2}\right) T_i^j + \frac{k\Delta t}{\rho c(\Delta l)^2} T_{i-1}^j + \frac{\Delta t}{\rho c} \frac{bP}{\sqrt{2\pi\sigma v}} \exp(-bi\Delta l) \exp\left(-\frac{(j\Delta t - \tau/2)^2}{2\sigma^2}\right) \quad (27)$$

After establishing the grid Fourier number $F_{0i} = \frac{k\Delta t}{\rho c(\Delta l)^2}$, Equation (27) could be transformed into the following form [25,26]:

$$T_i^{j+1} = F_{0i} T_{i+1}^j + (1 - 2F_{0i}) T_i^j + F_{0i} T_{i-1}^j + \frac{\Delta t}{\rho c} \frac{bP}{\sqrt{2\pi\sigma v}} \exp(-bi\Delta l) \exp\left(-\frac{(j\Delta t - \tau/2)^2}{2\sigma^2}\right) \quad (28)$$

Appendix B (Number to be taken over from the main text)

Experiment for Ultrasonic cleaning

In order to reduce the influence of impurities such as droplets and dust on the observation results, the experimental acrylic sheets were placed in

the ultrasonic cleaner and cleaned with purified water before laser ablation of PMMA materials and surface topography detection. The experimental ultrasonic cleaning machine (Model: Yujie AK-100SD) has an ultrasonic power of 900 W, a heating power of 600 W, and a working frequency of 40 kHz. During the process of cleaning acrylic sheets, the machine heating switch was turned on, the cleaning temperature and the cleaning time was set to 30 °C and 10 minutes, respectively, and the cleaning ultrasonic power was adjusted to five levels, approximately 900 W. In the process of CO₂ continuous laser ablation of PMMA sheet, polymethyl methacrylate was heated and decomposed into methyl methacrylate monomer under the action of high-energy laser beam. Methyl methacrylate monomer is slightly soluble in water [30], therefore during the ultrasonic vibration process of the ultrasonic cleaning equipment, the monomer powder fell off the surface of PMMA sheet and entered the water due to vibration, causing the water to become turbid, and most of it condensed into blocks and floated on the surface of the water. It can be seen from Figure 17 that after ultrasonic cleaning of PMMA sheet after CO₂ continuous laser ablation, the impurity particles attached to the surface of the hole of PMMA sheet due to laser action were cleaned, and laser ablation marks were exposed. After the dirt on the surface of the board was thoroughly removed, it was dried to ensure that there were no water stains on the surface.

Processing parameters	Before Ultrasonic Cleaning	After Ultrasonic Cleaning
Laser power density 20 W/mm ² Laser beam movement speed 30 mm/s		
Laser power density 20 W/mm ² Laser beam movement speed 60 mm/s		
Laser power density 20 W/mm ² Laser beam movement speed 90 mm/s		

(a) Laser power density of 23.3 W/mm²

Processing parameters	Before Ultrasonic Cleaning	After Ultrasonic Cleaning
Laser power density 60 W/mm ² Laser beam movement speed 30 mm/s		
Laser power density 60 W/mm ² Laser beam movement speed 60 mm/s		
Laser power density 60 W/mm ² Laser beam movement speed 90 mm/s		

(c) Laser power density of 69.9 W/mm²

Processing parameters	Before Ultrasonic Cleaning	After Ultrasonic Cleaning
Laser power density 40 W/mm ² Laser beam movement speed 30 mm/s		
Laser power density 40 W/mm ² Laser beam movement speed 60 mm/s		
Laser power density 40 W/mm ² Laser beam movement speed 90 mm/s		

(b) Laser power density of 46.6 W/mm²

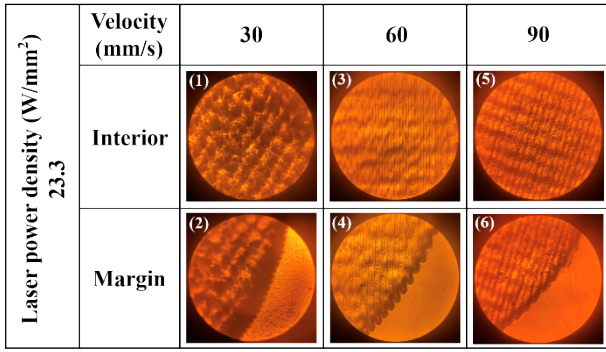
Processing parameters	Before Ultrasonic Cleaning	After Ultrasonic Cleaning
Laser power density 80 W/mm ² Laser beam movement speed 30 mm/s		
Laser power density 80 W/mm ² Laser beam movement speed 60 mm/s		
Laser power density 80 W/mm ² Laser beam movement speed 90 mm/s		

(d) Laser power density of 93.2 W/mm²

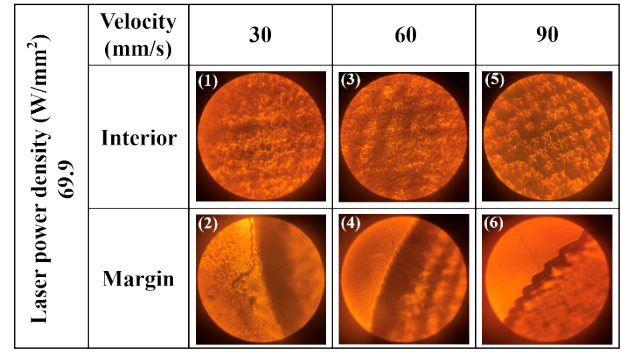
Figure S17 Ultrasonic cleaning effect under different laser process parameters

Appendix C (Number to be taken over from the main text)

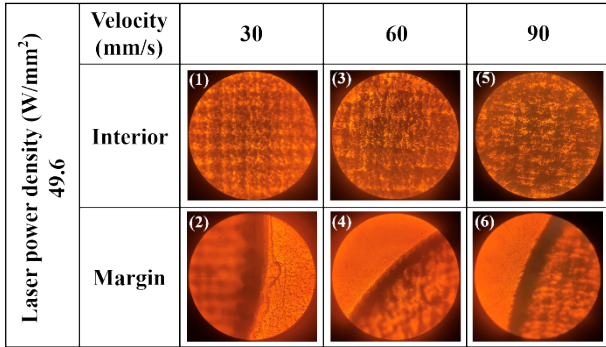
Complete data and images



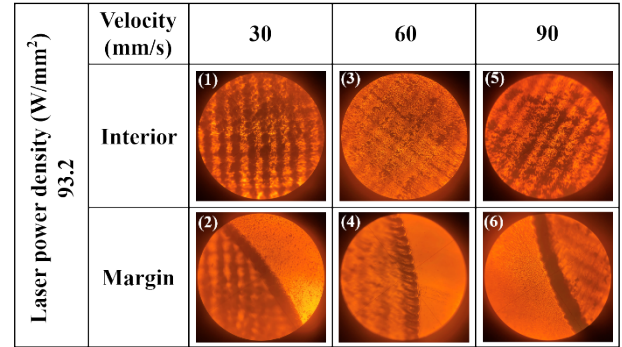
(a) Laser power density of 23.3 W/mm²



(c) Laser power density of 69.9 W/mm²



(b) Laser power density of 46.6 W/mm²



(d) Laser power density of 93.2 W/mm²

Figure S18 Surface morphology of PMMA sheet observed under low-pressure mercury/sodium lamp with optical microscope

Table S9 Surface roughness values under different laser process parameters

Laser power density (I ₀)/(W/mm ²)	Laser beam moving velocity (v)/(mm/s)	Surface roughness values (Ra)/μm				Average value
		Measurement point 1	Measurement point 2	Measurement point 3	Measurement point 4	
23.3	30	5.79	5.22	4.21	5.99	5.30
	60	9.89	5.02	4.99	9.89	7.45
	90	4.46	4.29	4.55	4.65	4.49
46.6	30	5.98	3.74	4.16	6.62	5.12
	60	12.41	5.54	9.82	9.33	9.27
	90	5.00	2.85	2.78	4.00	3.66
69.9	30	5.98	4.21	4.34	5.67	5.05
	60	11.44	8.33	4.48	12.63	9.22
	90	6.09	4.47	3.51	4.90	4.74
93.2	30	5.84	4.80	3.95	6.43	5.25
	60	12.05	6.59	5.06	13.23	9.23
	90	4.25	3.76	2.41	3.33	3.43